Cureus
Part of SPRINGER NATURE

Open Access Original Article

Curcumin Modulates Viability and Apoptosis-Associated Transcripts in HepG2 Cells

Fatima A. Al-Derwish [1], Abdalla R. ElGenaidi [2], Abdalla A. Elamin [3], Faris Abdon [4], Emhemed R. Abukhattala [5], Ayman B. Mustafa [6], Adil Khalil Hussien Khalil [7]

1. School of Basic Sciences, Libyan Academy for Postgraduate Studies, Misurata, LBY 2. Medical Genetics, Faculty of Health Sciences, Misurata University, Misurata, LBY 3. Department of Anatomy, RAK Medical and Health Sciences University, Ras Al Khaimah, ARE 4. Medical Sciences Department/Medical Biochemistry Unit, Orotta College of Medicine and Health Sciences, Asmara, ERI 5. Life Sciences, Libyan Academy for Postgraduate Studies, Misurata, LBY 6. Therapeutic Nutrition, Faculty of Health Sciences, Misurata University, Misurata, LBY 7. College of Medicine, Basic Medical Science Department, Dar Al Uloom University, Riyadh, SAU

Corresponding author: Faris Abdon, farismabdon@gmail.com

Review began 10/27/2026
Review ended 11/06/2026
Published 11/10/2026

© Copyright 2026
Al-Derwish et al. This is an open access article distributed under the terms of the Creative Commons Attribution License CC-BY 4.0., which permits unrestricted use, distribution, and reproduction in any medium, provided the original author and source are credited.

DOI: 10.7759/cureus.119424

Abstract

Introduction

Curcumin, the principal curcuminoid of turmeric (*Curcuma longa*), has shown growth-inhibitory activity in hepatocellular carcinoma (HCC) models. This study examined metabolic viability, cell morphology, death-mode distribution, and apoptosis-associated transcripts in HepG2 cells exposed to curcumin within a single time-resolved protocol.

Methods

HepG2 cells were exposed to curcumin at 17.0-542.9 µM for 24, 48, or 72 hours. Metabolic viability was measured by the 3-(4,5-dimethylthiazol-2-yl)-2,5-diphenyltetrazolium bromide (MTT) assay, and the 50% inhibitory concentration (IC_{50}) at each exposure time was estimated by nonlinear regression. Morphology was examined by hematoxylin and eosin staining, and death-mode distribution by acridine orange/ethidium bromide (AO/EB) staining at the time-matched IC_{50}. After 48 hours at the 48-hour IC_{50}, the relative *p53*, *BAX*, and *BCL-2* mRNA expression was measured by quantitative real-time polymerase chain reaction (qPCR). Each endpoint was measured in a single experimental series, with three technical replicate wells per MTT condition and technical duplicate qPCR reactions.

Results

The MTT-derived IC_{50} values were 490.3 µM at 24 hours, 34.9 µM at 48 hours, and 49.0 µM at 72 hours, and the concentration effect on viability was significant at each exposure time (one-way analysis of variance, $P < 0.001$). Treated cells showed reduced confluence, shrinkage, rounding, detachment, and cellular debris. On AO/EB staining, live cells accounted for 97% of untreated cells and for 75%, 62%, and 57% of cells after 24, 48, and 72 hours at the time-matched IC_{50}, with apoptotic fractions (24-33%) exceeding necrotic fractions (1-10%). After 48 hours, relative to untreated cells and normalized to glyceraldehyde-3-phosphate dehydrogenase, *p53* and *BAX* mRNA expression was 1.87- and 1.50-fold, and *BCL-2* mRNA expression was 0.76-fold; the *BAX/BCL-2* transcript ratio, which does not depend on the reference gene, was 1.9-fold higher.

Conclusions

In HepG2 cells, curcumin reduced MTT-based metabolic viability, and this reduction was accompanied by morphological changes, an AO/EB distribution shifted toward apoptotic cells, and a higher *BAX/BCL-2* transcript ratio. These single-series in vitro observations describe a growth-inhibitory response with apoptosis-associated features and provide a basis for replicated, protein-level studies in additional hepatic cell models.

Categories: Pharmacology, Integrative/Complementary Medicine, Oncology
Keywords: apoptosis, bax/bcl-2 ratio, curcumin, hepatocellular carcinoma, hepg2 cells, mtt assay, p53

Introduction

Hepatocellular carcinoma (HCC) is the predominant histologic type of primary liver cancer and a major global health problem. Global Cancer Observatory (GLOBOCAN) 2022 estimated approximately 866,000 new liver cancer cases and 758,000 liver cancer deaths worldwide, ranking liver cancer sixth in incidence and third in cancer mortality [1]. HCC accounts for approximately 90% of primary liver cancers [2]. Five-year survival for HCC is approximately 20% or less in most population-based series [3]. Many patients are diagnosed at intermediate or advanced stages, when curative options are limited, and recurrence, tumor heterogeneity, drug resistance, and treatment-related toxicity continue to limit durable disease control

[2,4,5].

Naturally derived bioactive compounds attract interest as anticancer candidates because of their multi-target biological effects in preclinical research [6,7]. Curcumin is the principal curcuminoid of the rhizome of *Curcuma longa* L. (turmeric; family Zingiberaceae) and is also present in related *Curcuma* species. It has been widely studied for its antioxidant, anti-inflammatory, and anticancer properties [7,8]. In liver cancer research, curcumin has shown pro-apoptotic, antiproliferative, anti-angiogenic, and anti-invasive effects, but its clinical translation is limited by poor oral bioavailability [7-9].

Curcumin has been reported to reduce viability, promote apoptosis-associated responses, and alter cell-cycle progression in HepG2 cells and other HCC models [10-15]. These effects have often been examined in separate experimental designs or with single endpoints. Measuring viability, morphology, death-mode distribution, and apoptosis-associated transcription within the same time-resolved HepG2 protocol allows these responses to be related to one another under matched exposure conditions.

The primary objective of this study was to describe the concentration- and time-dependent effect of curcumin on the metabolic viability of HepG2 cells, measured by the 3-(4,5-dimethylthiazol-2-yl)-2,5-diphenyltetrazolium bromide (MTT) assay after 24, 48, and 72 hours of exposure. The secondary objectives were to describe, under conditions defined by the MTT-derived 50% inhibitory concentration (IC_{50}), cell morphology on hematoxylin and eosin (H&E) staining, death-mode distribution on acridine orange/ethidium bromide (AO/EB) staining at the time-matched IC_{50}, and relative *p53*, *BAX*, and *BCL*-2 mRNA expression measured by quantitative real-time polymerase chain reaction (qPCR) at the 48-hour IC_{50}.

Materials And Methods

Study design

This in vitro experimental study evaluated the effects of curcumin on HepG2 human hepatoma cells. Dose-response experiments were performed after 24, 48, and 72 hours of curcumin exposure. Transcript analysis was performed at the 48-hour MTT-derived IC_{50}, corresponding to 34.9 µM (12.84 µg/mL). The study used an established, commercially available human cell line and did not involve human participants or animals; ethics committee approval was therefore not required.

Materials and reagents

Curcumin powder (98% purity) was supplied by Wuxi Hongmeirui Medical Technology Co., Ltd. (Wuxi, China). RPMI-1640 medium and 0.25% trypsin-EDTA were purchased from Biowest (Nuaillé, France). Dimethyl sulfoxide (DMSO), fetal bovine serum (FBS), and MTT were obtained from Sigma-Aldrich (St. Louis, MO, USA). Acridine orange and ethidium bromide were obtained from Merck KGaA (Darmstadt, Germany). TransZol reagent was obtained from TransGen Biotech (Beijing, China). The RevertAid First Strand cDNA Synthesis Kit and Maxima SYBR Green qPCR Master Mix were obtained from Thermo Fisher Scientific (Waltham, MA, USA).

Cell line and culture conditions

HepG2 cells, a human hepatoma cell line derived from the liver tumor of a 15-year-old male, were obtained from the American Type Culture Collection (ATCC; Manassas, VA, USA) and cultured in RPMI-1640 medium supplemented with 10% FBS and 1% penicillin-streptomycin in a humidified incubator at 37°C with 5% CO_2. At approximately 80-90% confluence, cells were washed with phosphate-buffered saline (PBS), detached with 0.25% trypsin-EDTA, neutralized with complete medium, counted, and reseeded as required. The culture medium was replaced every two to three days.

Preparation of curcumin and treatments

Curcumin powder was dissolved in DMSO to obtain a 20 mg/mL stock solution (approximately 54.3 mM, based on a molecular weight of 368.38 g/mol). The stock was added to complete culture medium at 1% (v/v) to give the highest working concentration of 200 µg/mL (542.9 µM), and the lower working concentrations were freshly prepared by dilution in complete culture medium. The final DMSO concentration therefore decreased in proportion to the curcumin concentration, from 1% at 542.9 µM to approximately 0.03% at 17.0 µM, and the 1% DMSO vehicle control corresponded to the highest solvent exposure. HepG2 cells were allowed to attach for 24 hours and were then exposed to curcumin at final concentrations of 17.0, 33.9, 67.9, 135.7, 271.5, and 542.9 µM (6.25, 12.5, 25, 50, 100, and 200 µg/mL, respectively) for 24, 48, or 72 hours, depending on the assay. Untreated cells cultured in medium alone and the 1% DMSO vehicle control were included.

MTT assay

HepG2 cells were seeded in 96-well plates at 1×10^4 cells/well, allowed to attach for 24 hours, and treated with curcumin or control conditions for 24, 48, or 72 hours. Each condition was tested in three technical

replicate wells at each exposure time within a single experimental series, with the well as the experimental unit. MTT stock solution (5 mg/mL in PBS) was diluted 1:10 in fresh RPMI-1640 medium immediately before use to give a working concentration of 0.5 mg/mL. At the end of each exposure period, the curcumin-containing medium was completely aspirated before MTT was added to limit interference of residual extracellular curcumin with the MTT readout. Working MTT solution (100 µL) was then added to each well, and plates were incubated for four hours at 37°C with 5% CO_2 to allow formazan crystal formation. The MTT solution was removed, 100 µL of DMSO was added to each well, plates were mixed for 10 minutes, and absorbance was measured at 570 nm, outside the main visible absorbance band of curcumin (approximately 408-500 nm), using a microplate reader (HUMAN Diagnostics Worldwide, Wiesbaden, Germany). The assay followed the method described by Mosmann [16]. Cell viability was calculated as follows:

$$\text{Viability (\%)} = (OD_{treated} / OD_{control}) \times 100,$$

where OD is the optical density and untreated cells served as the control. Dose-response curves were fitted by nonlinear regression, and IC_{50} values were obtained from the fitted curves as point estimates of 50% inhibition of metabolic viability.

Morphological assessment by H&E staining

HepG2 cells were seeded in six-well plates, allowed to attach for 24 hours, and treated with curcumin at 17.0, 33.9, 67.9, or 135.7 µM (6.25, 12.5, 25, or 50 µg/mL, respectively), alongside untreated and 1% DMSO vehicle-control cells, for 24, 48, or 72 hours. After treatment, cells were washed with PBS, passed through graded ethanol, stained with hematoxylin for five minutes, rinsed with distilled water, counterstained with eosin for two minutes, washed, and dehydrated through graded ethanol. Representative fields were photographed under a light microscope with 20× and 40× objectives, and morphology was assessed qualitatively.

AO/EB fluorescence staining

HepG2 cells were seeded on eight-well chamber slides (SPL Life Sciences, Pocheon, South Korea) at 2×10^4 cells/well. After attachment, cells were treated with curcumin at the time-matched IC_{50}: 490.3 µM (180.6 µg/mL) for 24 hours, 34.9 µM (12.84 µg/mL) for 48 hours, and 49.0 µM (18.04 µg/mL) for 72 hours. Cells were then stained with equal volumes of acridine orange (100 µg/mL) and ethidium bromide (100 µg/mL) in PBS and examined under a fluorescence microscope (Axio Imager Z2; Carl Zeiss Microscopy, Jena, Germany). Ethidium bromide was handled as a mutagen with appropriate protective and waste-disposal procedures. Cells were classified manually by fluorescence appearance as viable (green), early apoptotic (yellow), late apoptotic (orange), or necrotic (red), and the percentage of each category was calculated as follows:

$$\text{Percentage (\%)} = (\text{number of cells in the category} / \text{total number of counted cells}) \times 100$$

RNA extraction, complementary DNA synthesis, and qPCR

HepG2 cells were treated for 48 hours with curcumin at the 48-hour IC_{50} (34.9 µM; 12.84 µg/mL), and untreated cells were processed in parallel. Total RNA was extracted with TransZol reagent by the phenol-chloroform method, and RNA quantity and purity were assessed with a NanoDrop ND-1000 spectrophotometer (Thermo Scientific, Wilmington, DE, USA). Complementary DNA (cDNA) was synthesized from 1 µg of total RNA with the RevertAid First Strand cDNA Synthesis Kit. Relative expression of *p53*, *BAX*, and *BCL-2* mRNA was measured with Maxima SYBR Green qPCR Master Mix on a DTlite real-time PCR system (DNA-Technology, Moscow, Russia), with *GAPDH* as the reference gene. The primer sequences are listed in Table *1*.

Gene	Forward primer (5′-3′)	Reverse primer (5′-3′)	Approximate amplicon size (bp)
p53	CAGCACATGACGGAGGTTGT	TCATCCAAATACTCCACACGC	200
BAX	TTTGCTTCAGGGTTTCATCC	CAGTTGAAGTTGCCGTCAGA	150
BCL-2	GGTGGGGTCATGTGTGTGG	CGGTTCAGGTACTCAGTCATCC	180
GAPDH	GAAGGTGAAGGTCGGAGTC	GAAGATGGTGATGGGATTTC	140

TABLE 1: Primer sequences used for quantitative real-time polymerase chain reaction

BAX: *BCL-2*-associated X protein; *BCL-2*: B-cell lymphoma 2; *GAPDH*: glyceraldehyde-3-phosphate dehydrogenase

Each 25 µL reaction contained 12.5 µL of 2× SYBR Green master mix, 1 µL of each primer, 1 µL of cDNA template (≤100 ng per reaction), and 10.5 µL of nuclease-free water. The analysis included one untreated and one curcumin-treated sample, and each reaction was run in technical duplicate. Relative expression was calculated by the $2^{-\Delta\Delta Cq}$ method [17], where $\Delta\Delta Cq = (Cq_{target} - Cq_{reference})_{treated} - (Cq_{target} - Cq_{reference})_{control}$, Cq is the quantification cycle, *GAPDH* is the reference gene, and untreated cells serve as the calibrator.

Statistical analysis

Data are presented as mean ± standard deviation (SD). Dose-response curves were fitted by nonlinear regression with a five-parameter logistic model, and IC_{50} values were estimated using GraphPad Prism version 10.3.1 (GraphPad Software, San Diego, CA, USA). For the MTT assay, the concentration effect at each exposure time was assessed by one-way analysis of variance (ANOVA) across the untreated control, the vehicle control, and the six curcumin concentrations, with three technical replicate wells per condition, followed by Tukey's multiple-comparisons test against the untreated control. The F statistic is reported for ANOVA and the studentized range statistic (q) for Tukey comparisons. MTT P values are based on between-well variation within a single experimental series. A two-sided $P < 0.05$ was considered statistically significant. AO/EB percentages and qPCR relative quantities were obtained from a single experimental series and are reported descriptively.

Results

MTT-based metabolic viability

Curcumin reduced the MTT-based metabolic viability of HepG2 cells at 24, 48, and 72 hours (Figure *1*). One-way ANOVA showed a concentration effect at each exposure time (24 hours: $F(7,16) = 7.16$, $P < 0.001$; 48 hours: $F(7,16) = 35.96$, $P < 0.001$; 72 hours: $F(7,16) = 30.23$, $P < 0.001$). Compared with untreated cells, viability was significantly lower at 542.9 µM after 24 hours, at 33.9-542.9 µM after 48 hours, and at all tested concentrations (17.0-542.9 µM) after 72 hours (Table *2*). The 1% DMSO vehicle control did not reduce viability relative to untreated cells at any exposure time. The IC50 values were 490.3 µM (180.6 µg/mL) at 24 hours, 34.9 µM (12.84 µg/mL) at 48 hours, and 49.0 µM (18.04 µg/mL) at 72 hours.

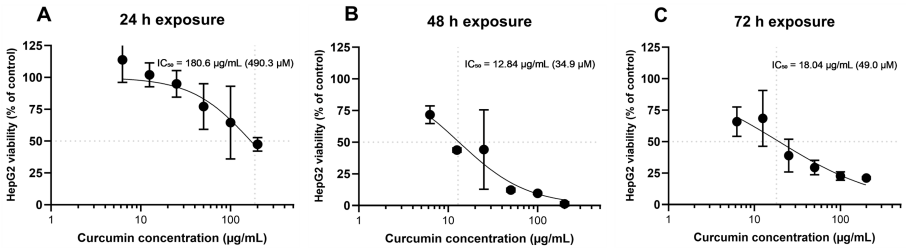


FIGURE 1: MTT-based metabolic viability of HepG2 cells after 24, 48, and 72 hours of curcumin exposure

Dose-response curves after 24 hours (A), 48 hours (B), and 72 hours (C) of exposure to curcumin at 17.0-542.9 µM (6.25-200 µg/mL; x-axis in µg/mL). Viability is expressed relative to untreated cells. Curves were fitted by nonlinear regression with a five-parameter logistic model; the IC_{50} shown in each panel is the point estimate for 50% inhibition of metabolic viability, and dotted lines mark 50% viability and the IC_{50}. Data are the mean ± SD of three technical replicate wells per condition.

MTT: 3-(4,5-dimethylthiazol-2-yl)-2,5-diphenyltetrazolium bromide; IC_{50}: 50% inhibitory concentration; SD: standard deviation

Exposure time	Condition	Viability (%), mean ± SD	Test statistic	P value
24 hours	All conditions (one-way ANOVA)	–	F(7,16) = 7.16	<0.001
	Untreated control (reference)	100.00 ± 0.22	–	–
	1% DMSO vehicle control	100.00 ± 0.19	q = 0.00	>0.999
	Curcumin 17.0 μM	113.84 ± 17.79	q = 1.65	0.930
	Curcumin 33.9 μM	102.00 ± 9.43	q = 0.24	>0.999
	Curcumin 67.9 μM	94.98 ± 10.49	q = 0.60	>0.999
	Curcumin 135.7 μM	77.17 ± 17.97	q = 2.73	0.553
	Curcumin 271.5 μM	64.51 ± 28.58	q = 4.24	0.116
	Curcumin 542.9 μM	47.43 ± 5.31	q = 6.28	0.008
48 hours	All conditions (one-way ANOVA)	–	F(7,16) = 35.96	<0.001
	Untreated control (reference)	100.00 ± 0.16	–	–
	1% DMSO vehicle control	100.00 ± 0.27	q = 0.00	>0.999
	Curcumin 17.0 μM	71.70 ± 6.95	q = 4.29	0.109
	Curcumin 33.9 μM	43.78 ± 1.69	q = 8.53	<0.001
	Curcumin 67.9 μM	44.25 ± 31.40	q = 8.46	<0.001
	Curcumin 135.7 μM	12.22 ± 1.52	q = 13.32	<0.001
	Curcumin 271.5 μM	9.61 ± 0.76	q = 13.71	<0.001
	Curcumin 542.9 μM	1.26 ± 1.70	q = 14.98	<0.001
72 hours	All conditions (one-way ANOVA)	–	F(7,16) = 30.23	<0.001
	Untreated control (reference)	100.00 ± 0.44	–	–
	1% DMSO vehicle control	100.00 ± 0.34	q = 0.00	>0.999
	Curcumin 17.0 μM	65.91 ± 11.65	q = 5.74	0.016
	Curcumin 33.9 μM	68.46 ± 22.25	q = 5.31	0.029
	Curcumin 67.9 μM	38.90 ± 13.00	q = 10.29	<0.001
	Curcumin 135.7 μM	29.38 ± 5.79	q = 11.90	<0.001
	Curcumin 271.5 μM	22.61 ± 3.33	q = 13.04	<0.001
	Curcumin 542.9 μM	21.12 ± 1.10	q = 13.29	<0.001

TABLE 2: MTT-based viability of HepG2 cells after 24, 48, and 72 hours of curcumin exposure

Viability values are mean ± SD of three technical replicate wells per condition, expressed relative to untreated cells. Statistical tests: at each exposure time, the eight conditions (untreated control, vehicle control, and six curcumin concentrations) were compared by one-way ANOVA (F statistic, F(7,16)), followed by Tukey's multiple-comparisons test of each condition against the untreated control (studentized range statistic, q(8,16)). P-values for the Tukey comparisons are multiplicity-adjusted. Curcumin concentrations of 17.0, 33.9, 67.9, 135.7, 271.5, and 542.9 μM correspond to 6.25, 12.5, 25, 50, 100, and 200 μg/mL, respectively.

MTT: 3-(4,5-dimethylthiazol-2-yl)-2,5-diphenyltetrazolium bromide; DMSO: dimethyl sulfoxide; SD: standard deviation; ANOVA: analysis of variance

Morphology on H&E staining

Untreated cells retained an adherent, epithelial-like appearance (Figure *2*). At 67.9 μM (25 μg/mL), curcumin-treated cells showed reduced confluence, shrinkage, rounding, partial loss of adhesion, and darker nuclear staining, particularly at 48 and 72 hours. At 135.7 μM (50 μg/mL), these features were more extensive, with greater detachment, lower cell density, and more cellular debris. Higher-magnification fields at all four H&E concentrations (17.0-135.7 μM) at 24 and 48 hours are provided in Appendix A.

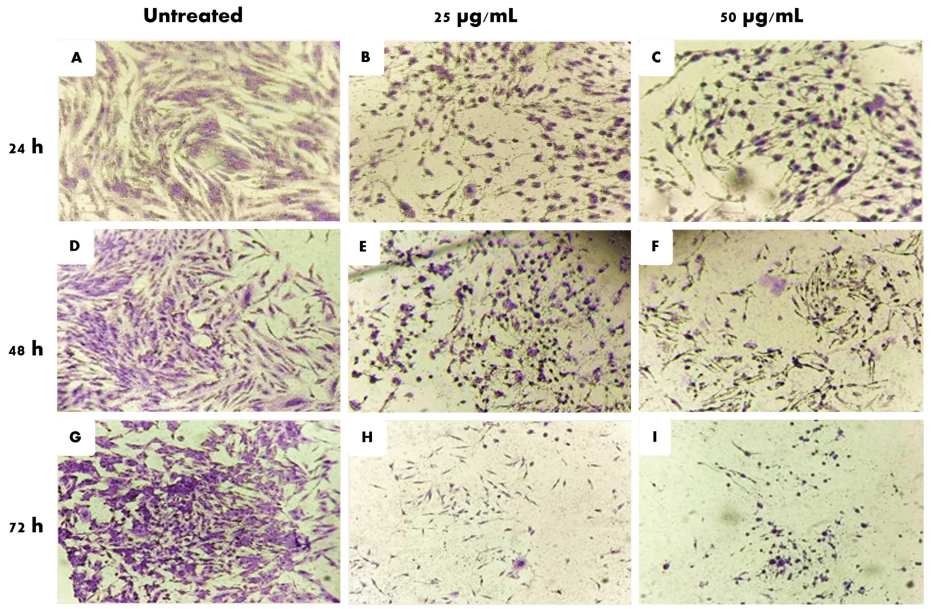


FIGURE 2: Hematoxylin and eosin morphology of HepG2 cells after curcumin exposure

Representative fields after 24 hours (A-C), 48 hours (D-F), and 72 hours (G-I) of exposure. Columns show untreated cells (A, D, G) and cells exposed to curcumin at 67.9 µM (25 µg/mL) (B, E, H) and 135.7 µM (50 µg/mL) (C, F, I). Original magnification, 20× objective. Higher-magnification (40×) fields are shown in Appendix A.

Death-mode distribution on AO/EB staining

Untreated cells were predominantly viable, with 97% live, 3% early apoptotic, 0% late apoptotic, and 0% necrotic cells (Figure 3). After curcumin exposure at the time-matched IC_{50}, live cells accounted for 75%, 62%, and 57% of cells at 24, 48, and 72 hours, respectively. Early apoptotic cells accounted for 20%, 25%, and 18%; late apoptotic cells for 4%, 8%, and 15%; and necrotic cells for 1%, 5%, and 10%. The combined apoptotic fraction (24%, 33%, and 33%) exceeded the necrotic fraction at each exposure time.

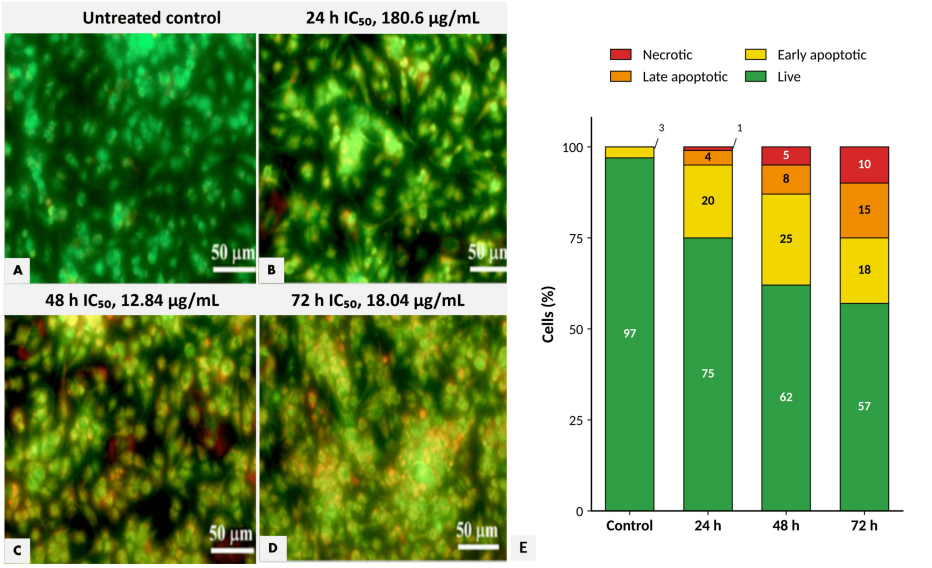


FIGURE 3: Acridine orange/ethidium bromide staining of HepG2 cells at the time-matched 50% inhibitory concentrations

Representative fields of untreated cells (A) and cells exposed to curcumin for 24 hours at 490.3 µM (180.6 µg/mL) (B), 48 hours at 34.9 µM (12.84 µg/mL) (C), and 72 hours at 49.0 µM (18.04 µg/mL) (D). Panel E shows the percentages of live (green), early apoptotic (yellow), late apoptotic (orange), and necrotic (red) cells for each condition.

Original magnification, 40× objective; scale bars = 50 µm. IC_{50}: 50% inhibitory concentration.

Apoptosis-associated transcript expression

After 48 hours of exposure at the 48-hour IC_{50}, GAPDH-normalized *p53* (1.87-fold) and *BAX* (1.50-fold) mRNA expression were higher, and *BCL-2* (0.76-fold) mRNA expression was lower in curcumin-treated cells than in untreated cells (Figure *4*). *GAPDH* Cq values were 0.85 cycles higher in treated samples (27.60 vs. 26.75), raw *p53* and *BAX* Cq values differed by less than 0.5 cycles between groups, and raw *BCL-2* Cq was 1.25 cycles higher in treated samples (Appendix B). The difference between *BAX* and *BCL*-2 Cq values, which does not depend on the reference gene, decreased from 1.00 in untreated to 0.05 in treated cells, corresponding to a 1.9-fold higher *BAX*/*BCL-2* transcript ratio. Quantification cycle values and relative expression calculations are provided in Appendix B.

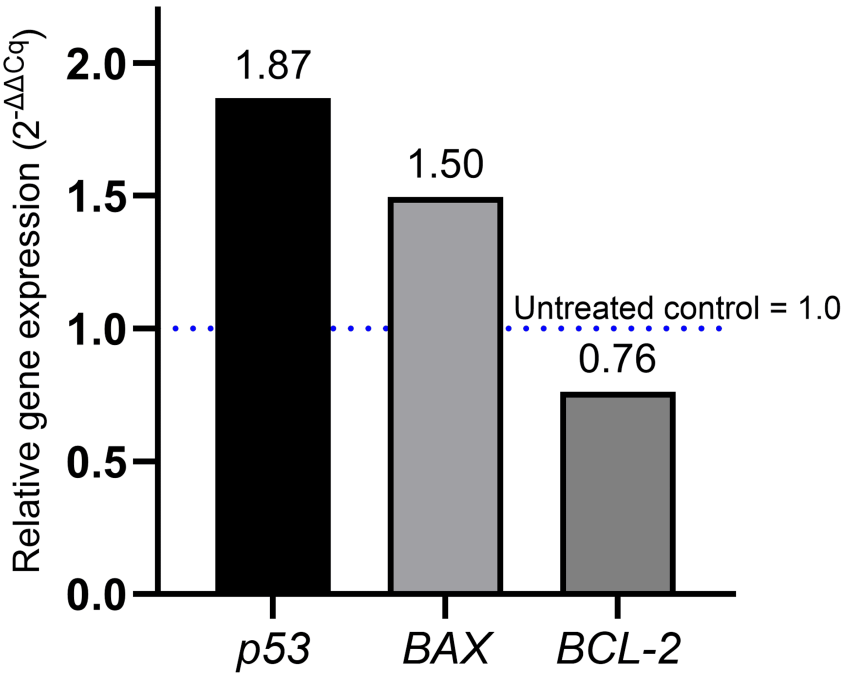


FIGURE 4: Relative expression of p53, BAX, and BCL-2 mRNA after 48 hours of curcumin exposure

HepG2 cells were exposed to curcumin at the 48-hour IC_{50} (34.9 µM; 12.84 µg/mL). Expression was normalized to *GAPDH* and calculated relative to untreated cells by the $2^{\Delta\Delta Cq}$ method. The dotted line marks the untreated control (calibrator) value of 1.0. Bars show the mean relative expression of technical duplicate reactions.

IC_{50}: 50% inhibitory concentration; *GAPDH*: glyceraldehyde-3-phosphate dehydrogenase; Cq: quantification cycle; *BAX: BCL-2*-associated X protein; *BCL-2*: B-cell lymphoma 2

Discussion

In this study, curcumin reduced the MTT-based metabolic viability of HepG2 cells at 24, 48, and 72 hours. The reduction was accompanied by morphological changes on H&E staining, a shift in AO/EB staining toward early and late apoptotic cells, and a higher *BAX/BCL-2* transcript ratio at the 48-hour IC_{50}. Together, these endpoints describe a growth-inhibitory response with apoptosis-associated features.

The viability findings agree with previous reports that curcumin suppresses HepG2 growth and promotes apoptosis-associated responses [10-15]. In the present study, metabolic viability, morphology, AO/EB classification, and selected apoptosis-related transcripts were measured within one time-resolved protocol, with death-mode analysis at time-matched IC_{50} concentrations, and the underlying viability data and Cq values are reported in full.

H&E staining showed reduced confluence, cell shrinkage, rounding, detachment, darker nuclear staining, and cellular debris, most evident at higher concentrations and longer exposures. Cell shrinkage, chromatin condensation, and nuclear pyknosis are classic features of apoptosis, whereas necrosis is more often associated with membrane disruption and uncontrolled cellular breakdown [18,19]. On AO/EB staining, the viable fraction decreased, and the early and late apoptotic fractions increased, while the necrotic fraction remained below the combined apoptotic fraction at every exposure time. This apoptosis-predominant distribution agrees with earlier studies in which curcumin promoted apoptosis in HepG2 cells and related liver cancer models [10,12,14,20].

The transcript findings were directionally consistent with the AO/EB observations. Curcumin-associated apoptosis in hepatic cancer cells has been linked to BAX/BCL-2 regulation, caspase activation, and reactive oxygen species-related signaling [12,20-22], and caspase-9 is a key initiator of the intrinsic mitochondrial apoptotic pathway [23]. In the present data, the higher *BAX/BCL-2* transcript ratio is independent of the reference gene, whereas the higher relative *p53* and *BAX* values arise from normalization to *GAPDH*, whose Cq values were higher in treated samples. These transcript changes are in the direction described for the intrinsic pathway; protein levels and caspase activity were not measured.

The IC_{50} decreased from 490.3 µM at 24 hours to 34.9 µM at 48 hours and was 49.0 µM at 72 hours; all three values were interpolated within the tested concentration range. At 24 hours, viability fell below 50% only at the highest concentration (47.43% at 542.9 µM), so the 24-hour estimate lies near the upper limit of the tested range, and between-well variability was greatest in this series (e.g., 64.51% ± 28.58% at 271.5 µM). The lower IC_{50} at 48 hours is consistent with a response that develops beyond the first 24 hours of exposure.

Curcumin degrades rapidly at physiological pH: about 90% decomposes within 30 minutes in phosphate buffer and serum-free medium at pH 7.2 and 37°C, and about half remains after eight hours in the medium containing 10% fetal serum [24,25]. The effective curcumin concentration therefore declines during prolonged exposure, and regrowth of surviving cells between 48 and 72 hours may account for the higher 72-hour IC_{50}. Curcumin stability in the culture medium was not measured in this study.

The micromolar concentrations used here exceed the circulating concentrations typically achieved after conventional oral curcumin administration [26]. The present findings therefore represent in vitro pharmacological effects, and formulation and delivery strategies that improve curcumin bioavailability remain relevant to translational work [27].

This study has limitations. It used a single liver cancer cell line, HepG2, which was originally described as hepatocellular carcinoma-derived and later characterized as hepatoblastoma-derived [28], and it did not include a non-malignant hepatic comparator, so cancer-cell selectivity was not assessed. MTT conditions were tested in technical replicate wells within one experimental series, and the AO/EB and qPCR analyses were each performed on a single sample per condition. MTT reduction reflects cellular metabolic activity rather than cell number, and curcumin's redox activity and visible-range absorbance can interfere with colorimetric and redox-based assays [25]; cell-free curcumin controls and orthogonal viability assays were not included. Apoptosis was assessed by AO/EB morphology and transcript levels; curcumin's intrinsic fluorescence overlaps the emission range of acridine orange [25], and annexin V/propidium iodide staining, caspase activity, and protein-level assays were not performed. The qPCR analysis used a single reference gene, *GAPDH*, whose stability under curcumin exposure was not assessed; primer amplification efficiencies and melt-curve data are not reported, and the $2^{-\Delta\Delta Cq}$ calculation assumes comparable amplification efficiencies for target and reference genes. Independent biological replicates, protein-level and functional apoptosis assays, validated reference genes, and additional hepatic cell models will extend these observations.

Conclusions

Curcumin reduced the MTT-based metabolic viability of HepG2 cells over 24 to 72 hours of exposure. At concentrations near the IC_{50}, this reduction was accompanied by morphological changes, an AO/EB distribution shifted toward early and late apoptotic cells, and a higher *BAX/BCL-2* transcript ratio. These single-series in vitro observations describe a growth-inhibitory response with apoptosis-associated features in HepG2 cells. Replicated experiments with protein-level and functional apoptosis assays, validated reference genes, and additional hepatic cell models will define the mechanisms underlying this response.

Appendices

Appendix A

Higher-magnification H&E fields of untreated, vehicle-control, and curcumin-treated HepG2 cells at all four H&E concentrations (17.0-135.7 µM) at 24 and 48 hours are shown in Figure *5*.

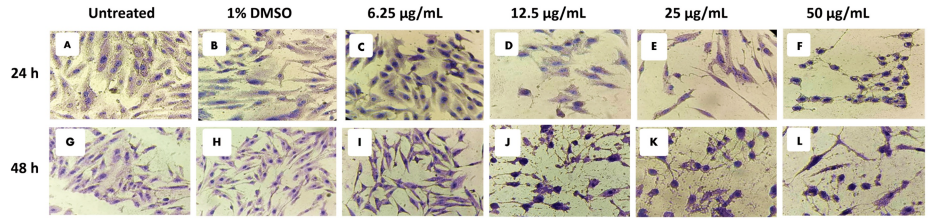


FIGURE 5: Higher-magnification hematoxylin and eosin morphology of HepG2 cells at 24 and 48 hours

Representative fields of untreated cells, 1% DMSO vehicle-control cells, and cells exposed to curcumin at 17.0 µM (6.25 µg/mL), 33.9 µM (12.5 µg/mL), 67.9 µM (25 µg/mL), and 135.7 µM (50 µg/mL) (columns, left to right) for 24 hours (A-F) and 48 hours (G-L). Original magnification: 40× objective.

DMSO: dimethyl sulfoxide

Appendix B

Quantification cycle values and relative expression calculations for the qPCR analysis are shown in Table 3.

Gene	Group	Reaction	Target Cq	GAPDH Cq	ΔCq	ΔΔCq	RQ ($2^{-\Delta\Delta Cq}$)
p53	Untreated	Duplicate 1	33.40	26.80	6.60	-0.15	1.1096
		Duplicate 2	33.60	26.70	6.90	0.15	0.9013
		Mean	33.50	26.75	6.75	0.00	1.0054
	Curcumin	Duplicate 1	33.60	27.80	5.80	-0.95	1.9319
		Duplicate 2	33.30	27.40	5.90	-0.85	1.8025
		Mean	33.45	27.60	5.85	-0.90	1.8672
BAX	Untreated	Duplicate 1	32.30	26.80	5.50	-0.05	1.0353
		Duplicate 2	32.30	26.70	5.60	0.05	0.9659
		Mean	32.30	26.75	5.55	0.00	1.0006
	Curcumin	Duplicate 1	33.10	27.80	5.30	-0.25	1.1892
		Duplicate 2	32.10	27.40	4.70	-0.85	1.8025
		Mean	32.60	27.60	5.00	-0.55	1.4959
BCL-2	Untreated	Duplicate 1	31.50	26.80	4.70	0.15	0.9013
		Duplicate 2	31.10	26.70	4.40	-0.15	1.1096
		Mean	31.30	26.75	4.55	0.00	1.0054
	Curcumin	Duplicate 1	32.90	27.80	5.10	0.55	0.6830
		Duplicate 2	32.20	27.40	4.80	0.25	0.8409
		Mean	32.55	27.60	4.95	0.40	0.7620

TABLE 3: Quantification cycle values and 2-ΔΔCq calculations after 48 hours of curcumin exposure

Curcumin-treated cells were exposed for 48 hours to the 48-hour IC50 (34.9 μM; 12.84 μg/mL). Each group represents one experimental sample measured in technical duplicate. ΔCq = target Cq − GAPDH Cq; ΔΔCq = ΔCq − mean ΔCq of the untreated sample; RQ = $2^{-\Delta\Delta Cq}$. Mean RQ is the arithmetic mean of the duplicate RQ values.

Cq: quantification cycle; RQ: relative quantity; GAPDH: glyceraldehyde-3-phosphate dehydrogenase; IC_{50}: 50% inhibitory concentration

Additional Information

Author Contributions

All authors have reviewed the final version to be published and agreed to be accountable for all aspects of the work.

Concept and design: Faris Abdon, Fatima A. Al-Derwish, Abdalla R. ElGenaidi, Abdalla A. Elamin, Emhemed R. Abukhattala, Ayman B. Mustafa

Acquisition, analysis, or interpretation of data: Faris Abdon, Fatima A. Al-Derwish, Abdalla R. ElGenaidi, Abdalla A. Elamin, Emhemed R. Abukhattala, Ayman B. Mustafa, Adil Khalil Hussien Khalil

Drafting of the manuscript: Faris Abdon, Abdalla A. Elamin, Emhemed R. Abukhattala, Ayman B. Mustafa, Adil Khalil Hussien Khalil

Critical review of the manuscript for important intellectual content: Faris Abdon, Fatima A. Al-Derwish, Abdalla R. ElGenaidi, Abdalla A. Elamin, Ayman B. Mustafa, Adil Khalil Hussien Khalil

Supervision: Abdalla R. ElGenaidi

Disclosures

Human subjects: All authors have confirmed that this study did not involve human participants or tissue. **Animal subjects:** All authors have confirmed that this study did not involve animal subjects or tissue. **Conflicts of interest:** In compliance with the ICMJE uniform disclosure form, all authors declare the following: **Payment/services info:** All authors have declared that no financial support was received from any organization for the submitted work. **Financial relationships:** All authors have declared that they have no financial relationships at present or within the previous three years with any organizations that might have an interest in the submitted work. **Other relationships:** All authors have declared that there are no other relationships or activities that could appear to have influenced the submitted work.

Acknowledgements

The authors thank their institutions for providing laboratory facilities and technical support.

References

1. Bray F, Laversanne M, Sung H, Ferlay J, Siegel RL, Soerjomataram I, Jemal A: Global cancer statistics 2022: GLOBOCAN estimates of incidence and mortality worldwide for 36 cancers in 185 countries. CA Cancer J Clin. 2024, 74:229-63. 10.3322/caac.21834
2. Llovet JM, Kelley RK, Villanueva A, et al.: Hepatocellular carcinoma. Nat Rev Dis Primers. 2021, 7:6. 10.1038/s41572-020-00240-3
3. Singal AG, Kanwal F, Llovet JM: Global trends in hepatocellular carcinoma epidemiology: implications for screening, prevention and therapy. Nat Rev Clin Oncol. 2023, 20:864-84. 10.1038/s41571-023-00825-3
4. Gao S, Jiang X, Wang L, Jiang S, Luo H, Chen Y, Peng C: The pathogenesis of liver cancer and the therapeutic potential of bioactive substances. Front Pharmacol. 2022, 13:1029601. 10.3389/fphar.2022.1029601
5. Llovet JM, Villanueva A, Lachenmayer A, Finn RS: Advances in targeted therapies for hepatocellular carcinoma in the genomic era. Nat Rev Clin Oncol. 2015, 12:408-24. 10.1038/nrclinonc.2015.103
6. Natu A, Singh A, Gupta S: Hepatocellular carcinoma: Understanding molecular mechanisms for defining potential clinical modalities. World J Hepatol. 2021, 13:1568-83. 10.4254/wjh.v13.i11.1568
7. Sharma RA, Gescher AJ, Steward WP: Curcumin: the story so far . Eur J Cancer. 2005, 41:1955-68. 10.1016/j.ejca.2005.05.009
8. Hewlings SJ, Kalman DS: Curcumin: a review of its effects on human health . Foods. 2017, 6:10.3390/foods6100092
9. Sharma S, Tanwar A, Gupta DK: Curcumin: an adjuvant therapeutic remedy for liver cancer . Hepatoma Res. 2016, 2:62-70. 10.20517/2394-5079.2015.59
10. Wang X, Tian Y, Lin H, Cao X, Zhang Z: Curcumin induces apoptosis in human hepatocellular carcinoma cells by decreasing the expression of STAT3/VEGF/HIF-1α signaling. Open Life Sci. 2023, 18:20220618. 10.1515/biol-2022-0618
11. Du Y, Xu B, Huang Y: Experimental study on the mechanism of curcumin inhibiting the proliferation of human hepatocellular carcinoma cells HepG2. BIO Web Conf. 2024, 111:02020. 10.1051/bioconf/202411102020
12. Huang Y: Inhibitory mechanism of curcumin on tumor cells . BIO Web Conf. 2024, 111:02024. 10.1051/bioconf/202411102024
13. Ren B, Luo S, Tian X, et al.: Curcumin inhibits liver cancer by inhibiting DAMP molecule HSP70 and TLR4 signaling. Oncol Rep. 2018, 40:895-901. 10.3892/or.2018.6485
14. Fan H, Tian W, Ma X: Curcumin induces apoptosis of HepG2 cells via inhibiting fatty acid synthase . Target Oncol. 2014, 9:279-86. 10.1007/s11523-013-0286-5
15. Zhang J, Liu Y, Wang X, Wang Z, Xing E, Li J, Wang D: Curcumin inhibits proliferation of hepatocellular carcinoma cells by blocking PTPN1 and PTPN11 expression. Oncol Lett. 2023, 26:307. 10.3892/ol.2023.13893
16. Mosmann T: Rapid colorimetric assay for cellular growth and survival: application to proliferation and cytotoxicity assays. J Immunol Methods. 1983, 65:55-63. 10.1016/0022-1759(83)90303-4
17. Livak KJ, Schmittgen TD: Analysis of relative gene expression data using real-time quantitative PCR and the 2(-Delta Delta C(T)) Method. Methods. 2001, 25:402-8. 10.1006/meth.2001.1262
18. D'Arcy MS: Cell death: a review of the major forms of apoptosis, necrosis and autophagy . Cell Biol Int. 2019, 43:582-92. 10.1002/cbin.11137
19. Newton K, Strasser A, Kayagaki N, Dixit VM: Cell death. Cell. 2024, 187:235-56. 10.1016/j.cell.2023.11.044
20. Yu J, Zhou X, He X, Dai M, Zhang Q: Curcumin induces apoptosis involving bax/bcl-2 in human hepatoma SMMC-7721 cells. Asian Pac J Cancer Prev. 2011, 12:1925-9.
21. Notarbartolo M, Poma P, Perri D, Dusonchet L, Cervello M, D'Alessandro N: Antitumor effects of curcumin, alone or in combination with cisplatin or doxorubicin, on human hepatic cancer cells. Analysis of their possible relationship to changes in NF-kB activation levels and in IAP gene expression. Cancer Lett. 2005, 224:53-65. 10.1016/j.canlet.2004.10.051
22. Zheng R, You Z, Jia J, et al.: Curcumin enhances the antitumor effect of ABT-737 via activation of the ROS-ASK1-JNK pathway in hepatocellular carcinoma cells. Mol Med Rep. 2016, 13:1570-6. 10.3892/mmr.2015.4715
23. Li P, Zhou L, Zhao T, et al.: Caspase-9: structure, mechanisms and clinical application . Oncotarget. 2017, 8:23996-4008. 10.18632/oncotarget.15098
24. Wang YJ, Pan MH, Cheng AL, Lin LI, Ho YS, Hsieh CY, Lin JK: Stability of curcumin in buffer solutions and characterization of its degradation products. J Pharm Biomed Anal. 1997, 15:1867-76. 10.1016/s0731-

7085(96)02024-9
25. Nelson KM, Dahlin JL, Bisson J, Graham J, Pauli GF, Walters MA: The essential medicinal chemistry of curcumin. J Med Chem. 2017, 60:1620-37. 10.1021/acs.jmedchem.6b00975
26. Garcea G, Jones DJ, Singh R, et al.: Detection of curcumin and its metabolites in hepatic tissue and portal blood of patients following oral administration. Br J Cancer. 2004, 90:1011-5. 10.1038/sj.bjc.6601623
27. Tabanelli R, Brogi S, Calderone V: Improving curcumin bioavailability: current strategies and future perspectives. Pharmaceutics. 2021, 13:10.3390/pharmaceutics13101715
28. López-Terrada D, Cheung SW, Finegold MJ, Knowles BB: Hep G2 is a hepatoblastoma-derived cell line . Hum Pathol. 2009, 40:1512-5. 10.1016/j.humpath.2009.07.003